ELSEVIER

Polymer 43 (2002) 1437–1446

polymer

www.elsevier.com/locate/polymer

Interfacial compatibilization for PSF/TLCP blends by a modified polysulfone

Jun Zhang, Jiasong He*

State Key Laboratory of Engineering Plastics, Center for Molecular Science, Institute of Chemistry, The Chinese Academy of Sciences, Beijing 100080, People's Republic of China

Received 16 March 2001; received in revised form 10 September 2001; accepted 21 September 2001

Abstract

Maleic anhydride-grafted polysulfone (PSF-*g*-MAH) was prepared by copolymerization in a solution. Compared to polysulfone, the surface tension and its polar fraction of PSF-*g*-MAH were increased by modification. The PSF-*g*-MAH was used to compatibilize polysulfone (PSF)/thermotropic liquid crystalline polymer (TLCP) (Vectra B950) blends. DRS–FTIR investigations showed that the special interaction between PSF and TLCP phases was enhanced due to the incorporation of PSF-*g*-MAH. The X-ray photoelectron spectroscopy (XPS) and PLM studies revealed that some chemical reactions had occurred between PSF-*g*-MAH and TLCP components, which produced PSF–VB copolymers. It is suggested that the improvement of compatibility should be attributed to some interactions including both chemical and physical ones. The improvement of compatibility was also confirmed by DMA and TGA analysis. Morphological observation showed that the addition of compatibilizer significantly reduced the size of the dispersed TLCP phase, and in case of injection molding, PSF-*g*-MAH promoted the TLCP fibrillation and improved their dispersion within the matrix. The processabilities of PSF/TLCP blends before and after compatibilization were investigated. It was found that the melt viscosities were increased by the addition of PSF-*g*-MAH, which also gave an evidence of the occurrence of interaction between phases.

Keywords: Liquid crystalline polymer; Blends; Interfacial compatibilization

1. Introduction

Polymer blending is a useful and attractive approach to obtain new polymeric materials with more balanced properties than their components. The thermotropic liquid crystalline polymers (TLCPs), especially wholly aromatic TLCPs, due to their outstanding properties, have been used as blending components to improve properties of other isotropic polymers. The pioneering work on polymer blends containing TLCP was reported in early 1980s by a number of research groups [1–3]. Since the publication of Kiss's paper in 1987 [4], this type of blends, referred to as 'in situ composites', has become one of the hot spots for scientific and industrial interests. At the early stage of research on in situ composites, most work has been conducted on the LCP microfibril formation related with the melt viscosity or viscosity ratio, composition and flow mode, etc. These results have been summarized and reviewed by several researchers in their well-organized reviews [5–10].

As reported previously, almost pairs of LCPs and thermoplastics are incompatible or immiscible, which often leads to weak interfacial interaction. Consequently, the addition of LCPs to thermoplastics results in significant increase of the modulus of the in situ composite, but the strengths are only slightly superior to those of the matrix polymers [11,12].The weak interfacial interaction between LCP fibrils and the matrix polymers limits the wider application of in situ composites. So it is understandable that the compatibilization in in situ composites becomes one of the most important aspects. In recent years a large amount of researches focused on the compatibilization in LCP blends has been published [13–38]. Generally, for effective stress transferring from the matrix to the reinforcement, it is necessary to introduce a sufficient interfacial adhesion between the reinforcing LCP fibrils and the reinforced thermoplastic resin. The compatibilization in in situ composites can be achieved by incorporation of physical and/or chemical interactions between the two phases. These techniques for compatibilization in in situ composites can be classified into three types: (1) the addition of a third component as a compatibilizer; (2) transesterification between matrix and TLCP; (3) the addition of a third

* Corresponding author. Tel.: +86-10-6261-3251; fax: +86-10-6255-9373.

E-mail address: hejs@sklep.icas.ac.cn (J. He).

0032-3861/02/$ - see front matter
PII: S0032-3861(01)00674-7

polymer into binary polymer blends. The differences between the first and third types are that in the former usually the third component is a pre-made compound (or polymer) and its fraction in compatibilized blends is often less than 10 wt%. While the third polymer used in ternary blends is an as-received commercial product and its content in ternary blends can be changed in a wide range for tailoring the properties of blends.

For immiscible polymer blends, using a third component as a compatibilizer is a common and effective method [39]. Many block or graft copolymers with functional groups offering specific interaction and/or chemical reaction with component polymers have been used as compatibilizers. They may be added separately to the blend or formed in situ by reactive processing. It is expected that the compatibilizer concentrates at the interfacial region and reduces the interfacial tension like an emulsifier. Adhesion may be enhanced through interpenetration and entanglements. This approach is also successfully utilized for the compatibilization in in situ composites. Generally, the third components include functionalized polymers, ionomer and graft or block copolymer consisting of segments whose chemical structure and solubility parameters are similar to those of the polymers being blended. A great number of papers focused on the compatibilization of functionalized polymers for in situ composites.

Baird et al. [13–15] firstly used a functionalized polypropylene, MAH-*g*-PP, as a compatibilizer for in situ composites based on polypropylene reinforced by different thermotropic LCPs such as Vectra A950, B950 and Rodrun LC-3000. They found that MAH-*g*-PP tended to improve the interfacial adhesion between the LCP and the matrix polymer, to result in a finer and uniform distribution of the dispersed LCP fibrils. As a consequence, a significant enhancement in both tensile modulus and strength was achieved in LCP/PP blends. However, they could not find direct evidence to confirm the reaction between MAH-*g*-PP and the LCP, therefore, they suggested that some specific interactions such as hydrogen bonding responsible for the compatibilization. More recently, Baird and his co-workers [16] investigated the compatibilization of a reactive terpolymer based on ethylene–acrylic ester–maleic anhydride in Nylon 11/LCP blends. Their results showed that a small amount of terpolymer added led to in situ composites with significantly higher modulus and strength along the machine/reinforcing direction and substantially higher strength and toughness along the transverse direction of injection molded parts. Furthermore, compatibilized by the terpolymer, the final injection molded articles displayed a smoother surface. These behaviors were attributed to enhanced fibrillation of the LCP and improved interfacial adhesion between the LCP fibrils and polymer matrix. Chang and his coworkers conducted an interesting study on compatibilization of compatibilizers with epoxide functionalities in LCP/PET blends [17]. The addition of these compatibilizers resulted in higher stiffness, strength and toughness of compatibilized LCP blends. It was suggested that an epoxy-*co*-PET-*co*-LCP mixed copolymer was in situ formed during the melt processing, which would reduce the interfacial tension between these phases and enhance the fibril formation. However, the formation of this copolymer, or particularly the reaction of epoxy with the LCP, was not proved. Only the reduction of the amount of epoxide groups was proved by infrared spectroscopy (IR). But as Chang et al. discussed in their paper that these epoxide groups might undergo hydrolysis and other unknown reactions. Seo reported the compatibilization of maleic anhydride-grafted ethylene–propylene–diene terpolymer (MAH-*g*-EPDM) in PA46/Vectra B950, PA6/Vectra B950, PBT/Vectra A950 blends and etc. [18–23]. They found that a fine fibril structure of LCP could be developed by a shear flow in a thermoplastic matrix, even though the viscosity of the matrix was lower than that of the dispersed LCP. It was believed that this phenomenon was resulted from the in situ compatibilization of MAH-*g*-EPDM. They suggested that some chemical reactions between MAH groups and some end-groups of the LCP, such as –OH and $-NH_2$ etc. were responsible for the compatibilization.

It should be noticed that fibrillation of LCP is conflict with the miscibility in in situ composites. Baird et al. [15] found that in samples with relatively high loadings of compatibilizer, the dispersed TLCP droplets were too small to fibrillate subsequently during the mould filling step. Chang et al. [24] also obtained similar results. Therefore, optimization of the interfacial properties is critical to the overall performance of the in situ composites.

Polysulfone is a high performance polymer possessing satisfactory heat-resistance, high dimensional stability and good mechanical property. On the other hand, polysulfone also has a number of deficiencies, such as poor processability and poor solvent resistance. Blending PSF with other polymers for improving its processability has been reported. Kim et al. [40] prepared PSF/Vectra A950 blends by melt extrusion, and investigated the rheological and thermal behavior, mechanical properties and morphology of the blends. They concluded that PSF was immiscible with Vectra A950, however, at post draw with high draw ratio, the blends showed higher mechanical properties than neat PSF. Golovoy and his coworkers [41] also concluded that the addition of LCP (Vectra A950) to PSF resulted in an increase in stiffness, a small increase in tensile strength, and a significant improvement in processability. More recently, Inoue et al. [42–47] synthesized a series of modified polysulfone with different functional groups, such as maleic anhydride-grafted PSF (PSF-*g*-MAH), phthalic anhydride-terminated PSF (PSF-PhAH), PSF-epoxy and PSF-triazine. They systemically studied morphologies and interfacial properties of PSF/PA and PSF/modified PSF, and concluded that all reactive blend systems were expected to yield PSF–PA block copolymers between functional groups of PSF with amino chain-end of polyamide 6 (PA), and produced PSF–PA block

copolymers located at interface and effectively reduced size of dispersed phases.

In present study, a maleic anhydride-grafted polysulfone (PSF-*g*-MAH) is synthesized and used to compatibilize PSF/LCP (Vectra B950, hereafter referred as VB) blends. The processability, thermal behavior, morphology and interfacial property of PSF/LCP blends with and without the compatibilizer are studied. Based on above researches, the main goal of this study is to interpret the compatibilization mechanism of maleic anhydride-grafted PSF for PSF/VB blends.

2. Experimental

2.1. Materials

Polysulfone (PSF) with an *IV* of 0.54 was produced by Shanghai Shuguang Chemical Factory, China.

The TLCP used in this work was a wholly aromatic poly(ester amide), a copolymer based on 2,6-hydroxy naphthoic acid (60%), terephthalic acid (20%), aminophenol (20%) produced by Hoechst Celanese Co. Its trade name is Vectra B950, hereafter in this paper referred as VB.

The modified PSF with functional group, maleic anhydride-grafted PSF (hereafter referred as PSF-*g*-MAH in this paper), was synthesized according to Ref. [42]. The amount of anhydride groups in PSF-*g*-MAH was ca. 0.82% determined by chemical titration.

2.2. Blending

Prior to melt blending all materials were dried at 90°C under vacuum for at least 12 h. Polymer blends containing various VB content were prepared by melt mixing with a mixer, Haake Rheomix 600, at 305°C for 10 min with the rotor speed of 50 rpm. Meanwhile, the processability of blend melts was evaluated by torque values recorded during melt processing. This measurement was conducted at the rotor speed of 50 rpm on a Haake Rheomix 600 equipped with a Haake RC90 Rheocord.

Injection molding was carried out by using a miniature injection molder (Mini-Max Molder, CS-183 MM, Custom Scientific Instruments Inc.) at 300°C.

2.3. Observation and characterization

2.3.1. Contact angle measurements

The contact angles of two liquids on PSF and PSF-*g*-MAH were measured using JY-82 goniometer (Chengde, China), two liquids were water (double distilled) and ethylene glycol. Each reading was repeated at least 20 times. PSF and PSF-*g*-MAH films prepared by the solution casting method in a solvent of chloroform were served as test samples. Surface tension and its polar and dispersive components were calculated according to Harmonic Mean Equation [48]. Polar and dispersive components of surface tension for selected liquids were also obtained from the same literature [48].

2.3.2. FTIR measurements

IR was used to characterize interfacial interaction in polymer blends and performed with a Perkin–Elmer FTIR system 2000 spectrometer. Due to the insolubility of LCP component in most organic solvents, diffuse reflectance spectra (DRS) technique was taken by using a Perkin–Elmer diffuse reflectance (PEDR) accessory. In order to obtain good DRS–FTIR spectra, powder samples for infrared measurement were carefully filed from polymer blends plaques.

2.3.3. X-ray photoelectron spectroscopy measurements

X-ray photoelectron spectroscopy (XPS) measurements were used to determine the interfacial chemical reaction between components and carried out on a VG ESCALab 220I-XL spectrometer with Al Kα as X-ray source. To determine the interfacial chemical reaction, an experiment was designed and performed as follows (Fig. 1). First, the melt VB was hot pressed into a flake; then the droplets of PSF and PSF-*g*-MAH solutions in chloroform were put onto two flakes of VB, respectively. Second, after the solvent was completely volatilized, the samples were treated on a hot stage at 230°C for 2 h. The heat-treated VB flakes were extracted with chloroform for 20 h to remove the unreacted PSF and PSF-*g*-MAH. After completely drying VB flakes, XPS study was carried out.

2.3.4. DMA

DMA measurements were carried with a Perkin–Elmer DMA-7 from room temperature to 220°C. All measurements were conducted in the dual cantilever mode with a frequency of 1 Hz and heating rate of 5°C min^{-1}.

2.3.5. TGA

Thermogravimetric analysis was carried out with a TA Instrument 2950 TGA HR, the TGA experiments were performed in a dynamic mode of 10°C min^{-1} up to 700°C in N_2 atmosphere.

2.3.6. Scanning electron microscope observation

The fracture surface of injection molded specimens was

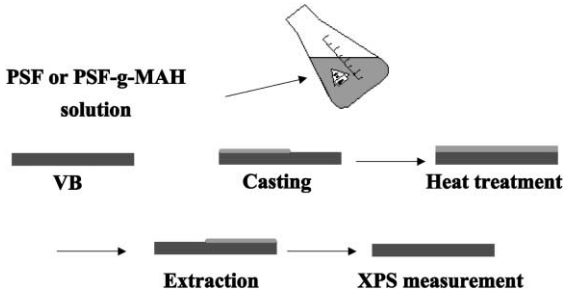

Fig. 1. A schematic of preparation of samples for XPS measurements.

Table 1
The contact angle data for PSF, PSF-*g*-MAH with water, ethylene glycol and resulting surface tension

Material	θ_1 (°)	θ_2 (°)	γ ($\times 10^{-3}$ N m^{-1})	γ^d ($\times 10^{-3}$ N m^{-1})	γ^p ($\times 10^{-3}$ N m^{-1})
PSF	79.8	52.5	37.7	26.0	11.7
PSF-*g*-MAH	38.0	25.1	65.0	34.4	30.6

obtained by immersing and breaking the samples in liquid nitrogen and coated with gold. Then the fracture surface of the blends was observed with a Hitachi S-530 scanning electron microscope (SEM).

2.3.7. PLM observation

After placing a piece of polymer blend sample on a piece of cover glass, and dropping appropriate amount of chloroform solvent onto the sample, the PSF and/or PSF-*g*-MAH could be dissolved in the solvent and became transparent amorphous thin film. The shape and size of dispersed VB particles in polymer blends could be maintained due to its insolubility in chloroform. By using PLM or contrast-phase optical microscopy, the VB particles dispersed within transparent matrix resin film were observed directly. The optical texture of LCP component was observed by a polarized optical microscope, Leica-DMLP (Leica Co.)

3. Results and discussion

3.1. Characterization of surface of modified polysulfone

After grafting maleic anhydride, the surface properties of polysulfone will be changed. Measurement of contact angle is a common method to evaluate the surface properties of polymers. This method consists of measuring the contact angle of two or more liquids on the surface of solid polymers. These liquids have known polar and dispersive components of the surface tension from specific handbooks. Then the contact angles can be used to calculate the surface tension of polymers. To perform this calculation, Harmonic Mean Equation can be used [48]

$$(1 + \cos\theta_1)\gamma_1 = 4\left(\frac{\gamma_1^d\gamma_s^d}{\gamma_1^d + \gamma_s^d} + \frac{\gamma_1^p\gamma_s^p}{\gamma_1^p + \gamma_s^p}\right)$$

$$(1 + \cos\theta_2)\gamma_2 = 4\left(\frac{\gamma_2^d\gamma_s^d}{\gamma_2^d + \gamma_s^d} + \frac{\gamma_2^p\gamma_s^p}{\gamma_2^p + \gamma_s^p}\right)$$

$$\gamma_i = \gamma_i^d + \gamma_i^p$$

where θ_1 and θ_2 are contact angles of liquid 1 and 2 on surface of a solid polymer, respectively, γ is surface tension of the polymer. Superscripts d and p represent dispersive component and polar component in surface tension. Using this equation, the data of surface tension of PSF and PSF-*g*-MAH was calculated. The data of contact angle of water, ethylene glycol on surface of PSF and PSF-*g*-MAH and calculated data of surface tension of PSF and PSF-*g*-MAH are listed in Table 1. From Table 1 it can be seen a sharp decrease in water contact angle of polymers after grafting, from 79.8 to 38.0°. The surface tension for PSF is 37.7×10^{-3} N m^{-1} and for PSF-*g*-MAH 65.0×10^{-3} N m^{-1}. Grafting maleic anhydride onto PSF increases the surface tension of the matrix by 27.3×10^{-3} N m^{-1} and increases the fraction of polar component in surface tension from 31 to 47%, which indicates grafting maleic anhydride onto PSF significantly increases fraction of polar component in surface tension. It should be noted that increasing polar component in surface tension favors the enhancement of the specific interaction between this polymer and other polar polymer components.

By using above described method, the data of surface tension of VB was also obtained. Combining surface tension of VB with those of PSF or PSF-*g*-MAH, the interfacial tension of PSF/VB and PSF-*g*-MAH/VB was further calculated. The calculated interfacial tension data can be used to predict the miscibilities of PSF/VB and PSF-*g*-MAH/VB. When using these techniques, it should be noticed that there are theoretical compromises or concerns. The first concern is that surface orientation of the injected samples used for contact angle measurements introduces some errors, because the surface energies of oriented and unoriented surface differ for TLCPs. The second concern is that reactions may occur between the two polymers, especially with the use of a compatibilizer. If the reactions at the interface occur, the contact-angle method would lead to overestimation of the interface tension. So, in the present study calculation of interfacial tension between VB and PSF or PSF-*g*-MAH has not been performed.

3.2. Interfacial characterization

3.2.1. FTIR studies

Improvement of miscibility in polymer blends often perturbs the environment of molecular chains of the blending polymer components, and causes changes in intensity and/or shifts of the characteristic absorption in IR spectra for polymer blends. This promises IR spectroscopy as a tool to characterize miscibility in polymer blends. FTIR was used to study miscibility of polystyrene/TLCP blends and light sulfonated polystyrene (SPS)/TLCP blends [35]. It was found that some characteristic absorption peaks shifted toward lower wave number in SPS/TLCP, caused by specific interactions between the carbonyl groups of TLCP and sulfonate groups of the acid form of SPS. Due to the insolubility of VB in almost all organic solvents, Diffuse

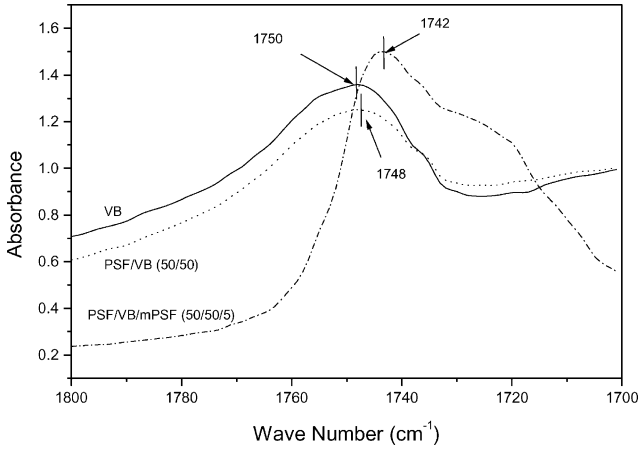

Fig. 2. The carbonyl stretch region of the FTIR spectra for neat VB and VB in PSF/VB blends.

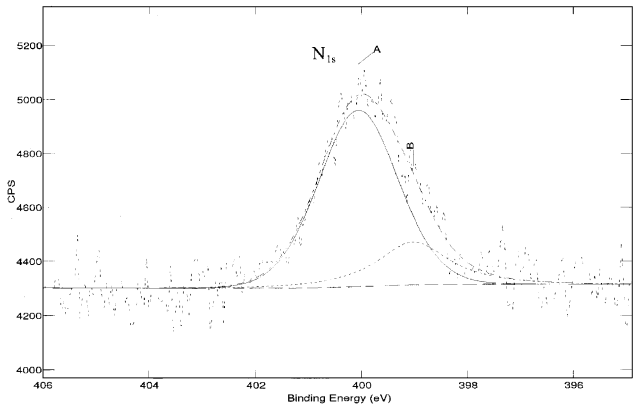

Fig. 3. The XPS spectrum of pure VB.

Reflection FTIR (DRIFT) was used to evaluate miscibility in this blend system.

The carbonyl stretch region of the spectra for neat VB and VB in PSF/VB blends without and with PSF-*g*-MAH (5 wt%) is shown in Fig. 2. It can be seen that the carbonyl stretch of VB locates at ca. 1750 cm^{-1}. After blending with PSF (50/50), the position of carbonyl stretch characteristic absorption retained, indicating no chemical changes or specific interactions had occurred, i.e. VB is immiscible with PSF at least at molecular level. While the incorporation of a small amount of PSF-*g*-MAH (5 wt%), the carbonyl absorption shifted to lower frequency, at ca. 1742 cm^{-1}. So it can be expected that the addition of PSF-*g*-MAH induces some specific interactions between phases.

Generally, in polar polymer blends, the specific interaction includes self-interaction and the interaction with other polymer, which can result in shifts of characteristic absorption for functional groups in IR spectrum. In this system of compatibilized PSF/VB blends, specific interaction may be enhanced by the addition of polar PSF-*g*-MAH, it should be noticed that the hydrogen bonding possibly forms between MAH and amino end-groups or hydroxyl end-group in VB, such as O–H–O hydrogen bonding. Baird et al. [18] also proposed that hydrogen bonding is the main compatibilization mechanism in PP/VA blends containing maleic anhydride-grafted PP.

There are several methods to determine the existence of the interfacial chemical reactions during melt blending, such as FTIR, selective extraction, NMR, GPC, XPS, and so on. Among these techniques, FTIR is one of most common and important methods. Chang et al. [49] studied PPO/PA blends compatibilized via SMA by means of FTIR. They found that characteristic adsorption peaks of $-\overset{O}{\overset{\|}{C}}-$ assigned to SMA at 1781 and 1857 cm^{-1} decreased drastically after melt blending with PA. This indicated that the anhydride group was involved in the chemical reaction. For the system used in this study, it is difficult to detect the change of intensity of some characteristic peaks by using FTIR, due to the small amount of anhydride groups in PSF-*g*-MAH chains and its dilution by blending. In addition, high absorptivity of VB dominating in this blend system is another difficulty to detect intensity change of maleic anhydride before and after melt blending.

3.2.2. X-ray photoelectron spectroscopy measurements

XPS is powerful to characterize the interfacial reaction between components in polymer blends. Fig. 3 shows N_{1s} detailed spectra of neat VB surface. It is seen that an asymmetric N_{1s} peak can further be fitted with two peaks, indicating there are two types of nitrogen atom in molecular chain of VB: one at 400.06 eV assigned to N in –NH–, and the other at 399.03 eV assigned to N in $-NH_2$. The XPS spectra of VB indicate the existence of a certain amount of $-NH_2$ end-groups. Therefore, when blending VB with PSF-*g*-MAH, the chemical reaction between maleic anhydride group and $-NH_2$ end-groups possibly occurred. In a further investigation, the N_{1s} spectrum for VB in PSF/VB and PSF-*g*-MAH/VB systems after heat treatment was measured. It has been found that the shape of N_{1s} peak in PSF/VB is similar to that of pure VB, and the shape of N_{1s} peak in PSF-*g*-MAH/VB becomes symmetrical (Fig. 4), which indicates that the terminal $-NH_2$ groups in VB have reacted with PSF-*g*-MAH and consumed during the heat treatment.

It is also possible to determine whether or not the interfacial reaction occurs by detecting the existence of sulfur, which belongs definitively to PSF covalently bonded to VB. The S_{2p} XPS spectrum of VB surface in PSF-*g*-MAH/VB system is shown in Fig. 5. Sulfur traces have been detected on VB side of PSF-*g*-MAH/VB blends after the extraction of PSF-*g*-MAH by chloroform, while no sulfur traces are found on VB side of PSF/VB binary blends, which further confirms that some chemical reactions have occurred between PSF-*g*-MAH and VB phases, and formed PSF–VB copolymers insoluble in chloroform.

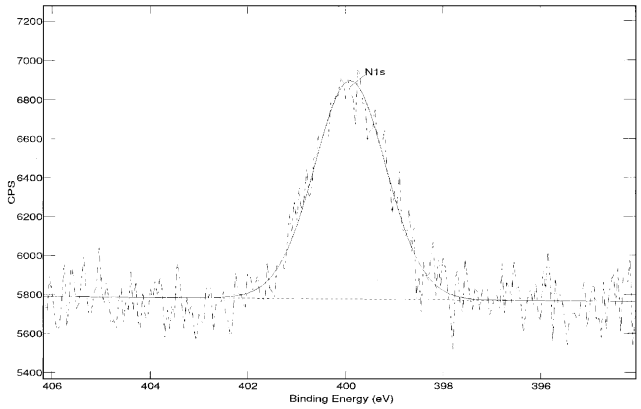

Fig. 4. The N_{1s} XPS spectrum of VB with PSF-*g*-MAH interface after heat treatment.

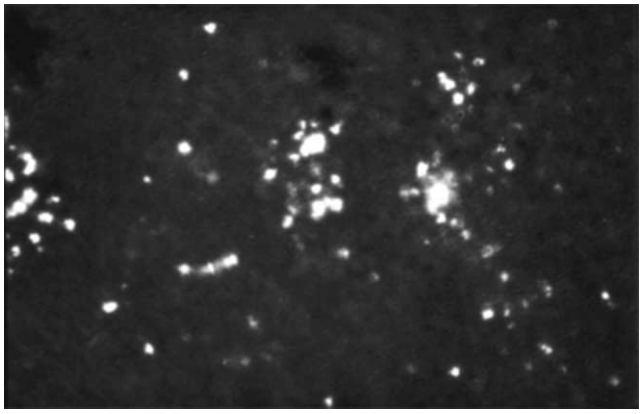

Fig. 6. The polarized light micrograph of the extract from PSF-*g*-MAH/VB (80/20).

3.2.3. PLM evidence for interfacial chemical reaction

Since the PSF is amorphous and dissoluble in chloroform, its thin film was casted from the extract of PSF/VB blend. Under crossed polarizers, its visual field is dark, indicating no chemical bonding between PSF and VB during melt blending. On the contrary, the thin film from the extract of PSF-*g*-MAH/VB blend exhibits birefringence patterns (see Fig. 6), attributed to optical feature of TLCP. This evidence confirms interfacial chemical reaction between PSF-*g*-MAH and VB yielding PSF–VB copolymers partially dissoluble in chloroform.

Previous studies have reported that polymers containing anhydride groups have been widely used as a compatibilizer to improve the interface adhesion of immiscible blends. For example, polypropylene-grafted with maleic anhydride (MAH) (PP-*g*-MAH) effectively improves the compatibility of PP/PA blends [37]. This is attributed to the reaction of maleic anhydride groups distributed along the PP-*g*-MAH backbone with amine groups located at the end of Nylon (PA) chains, and in situ formation of PP–PA copolymers. This copolymer can act as an emulsifier at the interface of PP and PA to reduce the interfacial tension and increase the interfacial adhesion as well as reduce the size of dispersed phase, thereby result in the improvement of mechanical properties of blends. In this system studied, VB contains not only amine end-groups but also some hydroxyl groups at the end of chains. During the melt blending, the chemical reactions would be possible as described in Fig. 7.

3.3. Morphological studies

Phase contrast microscopy has been used to observe the size and shape of dispersed TLCP phase in polymer blends in the present study. VB cannot be dissolved in most organic solvents, and the PSF has a good solubility in some polar organic solvents, such as chloroform, DMF. During extrusion or injection molding, under shear force, the orientation and fibrillation of the VB phase often occur and the deformation of VB phases possibly affects the judgment for

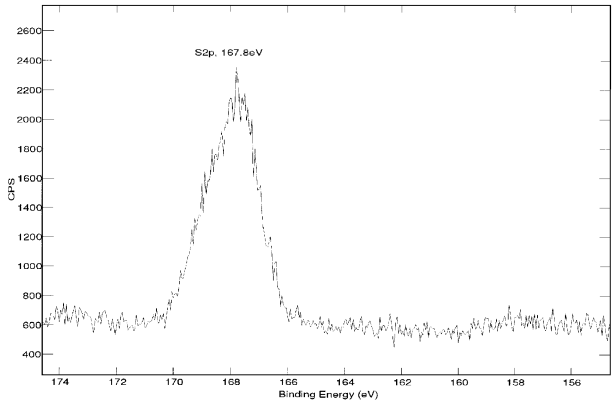

Fig. 5. The S_{2p} XPS spectrum of VB with PSF-*g*-MAH interface after heat treatment.

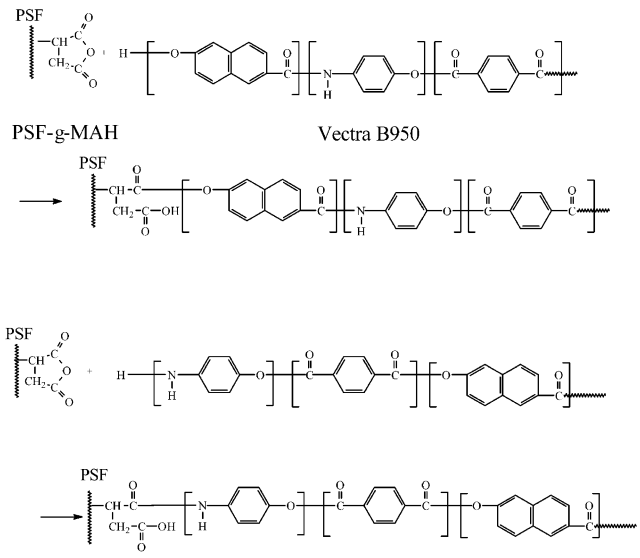

Fig. 7. Scheme of possible interfacial chemical reactions between PSF-*g*-MAH and VB during melt processing.

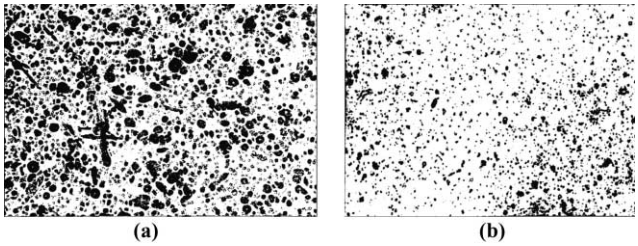

Fig. 8. Phase-contrast optical micrographs of: (a) PSF/VB (80/20) and (b) PSF/VB/PSF-*g*-MAH (80/20/5) (magnification is 400).

the miscibility of polymer blends. Therefore, the samples for optical microscopy observation were taken from blends prepared in a Haake Mixer. After the extraction of polysulfone in PSF/VB blends using chloroform, the insoluble VB particles can be directly observed under optical microscopy. Recently, the quantification of micrographs has been revolutionized by the advent of digital image-acquisition and image-processing techniques. In this work, after image processing through enhancing the phase contrast, a binary image with distinct light–dark differences between the two phases is obtained. The dispersion of VB component of PSF/VB (80/20) without and with PSF-*g*-MAH (5 wt%) is shown in Fig. 8. It is very clear that the addition of a small amount of PSF-*g*-MAH significantly reduces the size of VB particles. Binarization of micrographs favors the quantitative size measurement. After counting VB particles and calculating the particle size, the curves for number frequency-size distribution of PSF/VB (80/20) blends with various contents of PSF-*g*-MAH (0, 5, 10 wt%) are obtained and shown in Fig. 9. It is seen that the addition of 5 wt% PSF-*g*-MAH into PSF/VB (80/20) results in VB particles of smaller average diameters with a narrower size distribution, compared with PSF/VB (80/20) blends. With the increasing content of PSF-*g*-MAH in PSF/VB (80/20) blends, the average diameters of VB particles decrease further.

Morphological studies have also been done via SEM. Injection molded specimens of both PSF/VB and compatibilized PSF/VB blends reveal a skin-core structure. The difference in morphologies is along the skin region. The broken surfaces along the skin region of PSF/VB blends without and with PSF-*g*-MAH (5 wt%) are shown in Fig. 10. At the concentration of 20 wt% TLCP, the photo (Fig. 10(a)) reveals spherical and ellipsoidal shape of VB domain embedded in the PSF matrix. These domains are in the range of 5–10 μm in the diameter and appear to be distributed unevenly in PSF matrix. On the contrary, SEM micrographs of fracture surfaces along the skin region of PSF/LCP/PSF-*g*-MAH blends (Fig. 10(b)) exhibit a good fibrillar structure of VB, and the VB microfibrils are a few microns in diameter. For reinforcing matrix polymer, TLCP fibrils are more effective than spherical domains. One of the most important features for in situ composites is their TLCP fibrillar structure. There are several factors influencing the fibrillation of TLCPs in the thermoplastic matrix. Some are characteristics of thermotropic TLCPs, others parameters relate to melt processing. It should be noted that after melt blending PSF and TLCP in a single-screw or twin-screw extruder, the morphology of fracture surface for extrudates showed good TLCP fibrillar morphology even without any extensional drawing. But the situation is very complicated in the case of injection molding. Due to the significant interfacial difference and poor interfacial adhesion between PSF and VB phases, in the short processing time during injection molding, TLCP droplets were difficult to deform into fibrils unless some other methods such as high shear rates, extensional flow, molding thin specimens, were performed. From SEM photographs, it can be concluded that the addition of compatibilizer promotes the fibrillation of

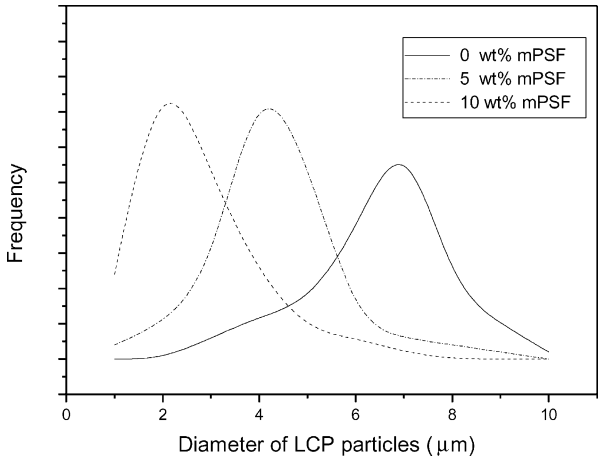

Fig. 9. Distribution of diameter of VB particles in PSF/VB (80/20) blends without and with PSF-*g*-MAH.

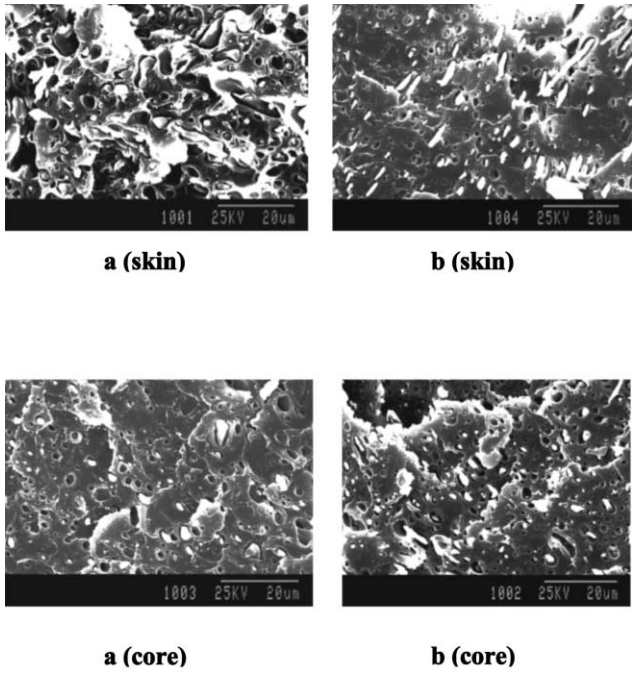

Fig. 10. Morphologies of fracture surfaces of blends: (a) PSF/VB 80/20, (b) PSF/VB/PSF-*g*-MAH 80/20/5.

TLCP and improved the distribution of TLCP fibrils within PSF matrix. The incorporation of PSF-*g*-MAH is believed to enhance shear stress transferring from matrix polymer to TLCP phase by reducing the interfacial tension and so promotes droplet deformation. At the meantime, the presence of PSF-*g*-MAH also provides a steric hindrance between dispersed VB particles and thus suppresses fibrils relaxation and coalescence.

3.4. Thermal properties

DMA methods have been extensively used for the analysis of the phase behavior of the polymer blends. This technique is usually more sensitive than DSC for detecting unclear transitions in some semi-crystalline polymers including most of TLCPs. In Fig. 11, E and tan δ are plotted as a function of temperature (in the range of 100–220°C) for PSF/VB (50/50) blends without and with 5 wt% PSF-*g*-MAH. It can be found that, in tan δ–T curves, all the materials analyzed show the presence of two transitions: the lower one associated with glass transition temperature of VB, and the higher one with that of PSF. It should be noticed that the values of T_g by DMA are slight higher than those obtained by DSC. Compared to a binary PSF/VB blend, the T_g of compatibilized blend shifts from 196 to 191°C. This is an evidence that the compatibility of PSF and VB is partially improved. However the T_g of VB in blend is little affected by the incorporation of the compatibilizer. In addition, a change in modulus is observed. Compatibilized blend exhibits higher modulus, which indicates an improvement of the compatibility resulting a stiffer blend. The same tendency is observed for other blends at various VB levels without and with compatibilizer.

As for the compatibilization effect on glass transition temperatures of components in in situ composites, it is of interest to pointed that several research groups [16,33] have found that compatibilization does not affect the transition temperatures of the respective components, while, other researchers [19,21,31,34] have reported that the incorporation of compatibilizers leads to obvious shifting of T_gs of TLCP and matrix polymer inward. Here, the authors believe that the effect of compatibilizer on position of T_gs is a reflection of compatibilization extent in polymer blends. Partial compatibilization by interfacial interaction often does not affect or only slightly affects the glass transition temperature of blending components, i.e. does not affect properties of bulk polymer components, although which significantly reduces the size of the dispersed phase and/or promote the fibrillation of TLCP components.

The TGA testing also can give a valuable information about the compatibility in polymer blends. The TG/DTG curves of neat PSF, VB and PSF/VB (50/50) blends without and with 5 wt% PSF-*g*-MAH are shown in Fig. 12. For binary PSF/VB blend, there are two major decomposition stages with peak temperatures at 517 and 534.6°C, respectively, having a difference of 17.6°C. After the addition of

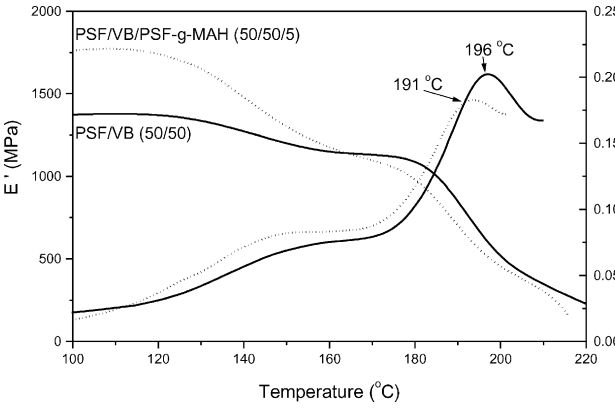

Fig. 11. The DMA spectra of PSF/VB (50/50) and PSF/VB/PSF-*g*-MAH (50/50/5).

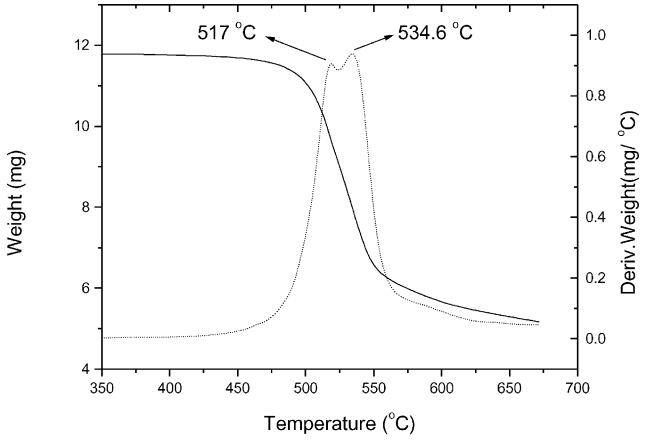

(a) PSF/VB (50/50)

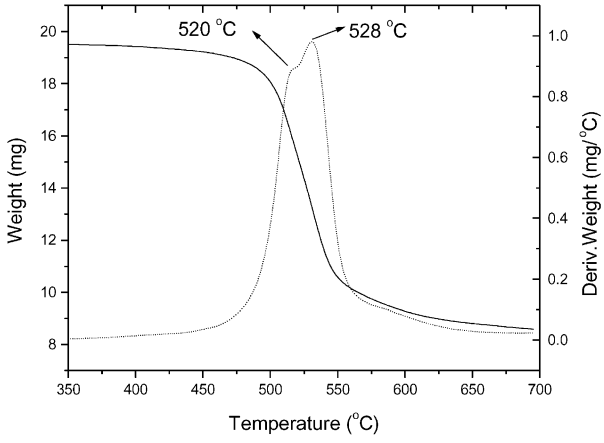

(b) PSF/VB/ PSF-g-MAH (50/50/5)

Fig. 12. The TG/DTG curves of PSF/VB (50/50) and PSF/VB/PSF-*g*-MAH (50/50/5).

the compatibilizer, the DTG curve of blend still shows two peaks, but the two peaks shift inward with a ΔT of 8°C; and, compared with the binary PSF/VB blend, the height of peak for VB component becomes smaller. This should be attributed to the dispersion uniformity of the dispersed phase resulted from improved compatibility. In the investigation of PA/VB compatibilized by EPDM-*g*-MAH by means of TGA technique, Seo et al. [21] obtained similar results.

3.5. Processabilities

Rheology has an important influence on the morphological structure formed during melt blending and can be used to a certain degree to judge whether a reaction is occurring in functionalized system. For non-reactive systems, melt viscosity (or torque recorded in the mixing experiment) is, to a first approximation, an additive property for blends. Polymer compatibilizing reactions between phases of interest here are expected to lead to an increase in the viscosity relative to this additive level and, with respect to processing time, depending on the rate of the reaction.

Fig. 13 shows a Haake torque experiment for the neat PSF, PSF/VB blends with and without PSF-*g*-MAH. In the first 5 min or so, the torque response is dominated by fluxing of the cold polymer pellets introduced into the heated chamber, after this stage, the torque of melt become steady. The viscosity of a PSF blend with 10 wt% VB was obviously lower than that of neat PSF, which consist with many reported results. The addition of small amounts of PSF-*g*-MAH to PSF/VB (90/10) raises the steady state torque. Similar results have also been observed for other PSF/VB blends with various compositions. At higher VB content, it should be noted that the mixing toques of compatibilized blends are slightly higher than those of corresponding blends without PSF-*g*-MAH. Increasing in melt viscosity implies that some interactions, including both chemical reactions and/or physical interactions, possibly occur due to the incorporation of PSF-*g*-MAH to PSF/VB system.

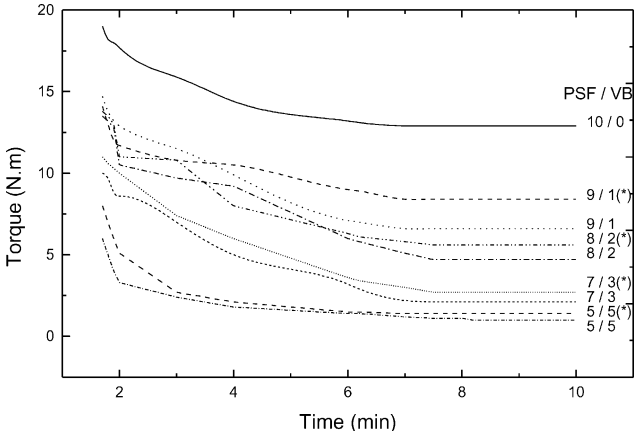

Fig. 13. The torque of PSF and its blends with VB (* containing 5 wt% PSF-*g*-MAH).

4. Conclusions

After grafting suitable functional groups, such us maleic anhydride, on polysulfone, the surface properties change obviously and exhibit increased surface tension. Especially, the polar fraction in surface tension increases more significantly, which provides a possibility to enhance the interfacial interactions with other polar components in polymer blends.

FTIR spectroscopy has been used to characterize the miscibility of polymer blends. For binary PSF/VB blends, the position of characteristic absorption for chemical groups in VB retains, which indicates no chemical changes or specific interactions occurred. While with the incorporation of a small amount of PSF-*g*-MAH, some characteristic absorptions shift to lower frequency, which implies the specific interactions of these functional groups may be involved. These interactions possibly include hydrogen bonding formed between MAH and amino end-groups or hydroxyl end-group in VB, such as O–H–O hydrogen bonding. However, using FTIR technique is difficult to find a direct evidence confirming the chemical reaction between PSF-*g*-MAH and VB.

There is a certain amount of $-NH_2$ end-groups contained in VB, confirmed by XPS. As a type of active chemical groups, $-NH_2$ end-groups may react with PSF-*g*-MAH during melt blending. N_{1s} spectrum for VB in PSF/VB and PSF-*g*-MAH/VB systems after heat treatment showed that the terminal $-NH_2$ groups of VB in PSF-*g*-MAH/VB system consumed during the heat treatment. Sulfur traces have been detected on VB side of PSF-*g*-MAH/VB blends after the extraction of PSF-*g*-MAH by chloroform, while no sulfur traces can be found on VB side of PSF/VB binary blends. Both N_{1s} and S detections indicate some chemical reactions occurred and PSF–VB copolymers yielded. PLM observation also gives an evidence confirmed interfacial chemical reaction between PSF-*g*-MAH and VB. Therefore, the improvement of compatibility should be attributed to both special interactions and interfacial chemical reactions.

The addition of a small amount of PSF-*g*-MAH significantly reduces the size of VB particles. With increasing content of PSF-*g*-MAH in PSF/VB (80/20) blends, the average diameters of VB particles further decrease. Both PSF/VB and compatibilized PSF/VB blends reveal a skin-core structure. The difference is that, in binary PSF/VB blends, the fracture surface reveals spherical and ellipsoidal structures of VB domain with large size. On the contrary, the fracture surfaces along the skin region of PSF/LCP/PSF-*g*-MAH blends exhibit a good fibrillar structure of VB with smaller diameters. It can be concluded that the addition of compatibilizer promotes the fibrillation of TLCP and improves the distribution of TLCP fibrils within PSF matrix.

The incorporation of PSF-*g*-MAH enhances shear stress transferring from matrix polymer to TLCP phase by reducing the interfacial tension and promotes droplet deformation. At the meantime, the presence of PSF-*g*-MAH also provides a steric hindrance between dispersed VB particles and thus suppresses fibrils relaxation and coalescence.

DMA analysis shows that compared to a binary PSF/VB blend, the T_g of PSF in compatibilized blends shifts to a lower temperature, which indicates a partially improved compatibility of PSF and VB. In addition, compatibilized blend exhibits higher modulus, which means the improvement of compatibility leads to a stiffer blend.

The TGA testing shows that the addition of PSF-*g*-MAH makes the two major decomposition peaks assigned to PSF and VB shift inward, which should be attributed to the dispersion uniformity of the dispersed phase resulted from improved compatibility.

The addition of small amounts of PSF-*g*-MAH to PSF/VB raises the steady state torque, implying that some interactions, including both chemical reactions and/or physical interactions, possibly occur.

Acknowledgements

This work is supported by National Natural Science Foundation of China, No. 59673022 and No. 50073027. The authors are also grateful for the fund support by Wang Kuan Cheng Education Foundation.

References

[1] Joseph EG, Wikes GL, Baird DG. Polym Prep 1983;24:304.
[2] Joseph EG, Wikes GL, Baird DG. Polym Prep 1984;25:94.
[3] Siegmann A, Dagan A, Kenig S. Polymer 1985;26:1325.
[4] Kiss G. Polym Engng Sci 1987;27:410.
[5] Brostow W. Polymer 1990;31:979.
[6] Dutta D, Fruitwala H, Kohli A, Weiss RA. Polym Engng Sci 1990;30:1005.
[7] La Mantia FP, Valenza A. Makromol Chem Macromol Symp 1992;56:151.
[8] Roetting O, Hinrichsen G. Adv Polym Technol 1994;13:57.
[9] Handlos AA, Baird DG. J Macromol Sci Rev Macromol Chem Phys 1995;C35:183.
[10] Isayev AI. In: Isayev AI, Kyu T, Cheng SZD, editors. Liquid-crystalline polymer systems, ACS symposium series, vol. 632. Washington, DC: ACS, 1996. Chapter 1.
[11] La Mantia FP, Valenza A, Magagnini PL. J Appl Polym Sci 1992;44:1257.
[12] Beery D, Kenig S, Siegmann A. Polym Engng Sci 1991;31:459.
[13] Datta A, Chen HH, Baird DG. Polymer 1993;34:759.
[14] Datta A, Baird DG. Polymer 1995;36:505.
[15] O'Donnell HJ, Baird DG. Polymer 1995;36:3113.
[16] Krishmaswarmy RK, Binwadud SE, Baird DG. Polymer 1999;40:701.
[17] Chin HC, Chion KC, Chang FC. J Appl Polym Sci 1996;60:2503.
[18] Seo Y. J Appl Polym Sci 1997;64:359–66.
[19] Seo Y, Hong SM, Kim KU. Macromolecules 1997;30:2978.
[20] Seo Y, Kim KU. Polym Engng Sci 1998;38:583.
[21] Seo Y. J Appl Polym Sci 1998;70:1589.
[22] Seo Y, Kim B, Kwak S, Kim KU, Kim J. Polymer 1999;40:4441.
[23] Seo Y, Kim B, Kim KU. Polymer 1999;40:4483.
[24] Chiou YP, Chiou KC, Chang FC. Polymer 1996;37:4099.
[25] Miller MM, Gowie JMG, Taid JG, Brydon DL, Mather RR. Polymer 1995;36:3107.
[26] Poli G, Paci M, Magagnini P. Polym Engng Sci 1996;36(9):1244.
[27] Grobelny J, Sek D. Polymer 1998;39:2143.
[28] Bruggeman A, Tinnemans AHA. J Appl Polym Sci 1999;71:1107.
[29] Wei KH, Tyan HL. Polymer 1998;39:2103.
[30] Wong SC, Mai YW, Leng Y. Polym Engng Sci 1998;38:156.
[31] Tjong SC, Li RKY, Xie XL. J Appl Polym Sci 2000;77:1964.
[32] Meng YZ, Tjong SC. Polymer 1998;39:99.
[33] Gopakumar TG, Ponrathnum S, Lele A, Rajan CR, Fradet A. Polymer 1999;40:357.
[34] Dutta D, Weiss RA, He JS. Polymer 1996;37:429.
[35] He JS, Liu J. J Appl Polym Sci 1998;67:2141.
[36] He JS, Liu J. Polymer 1999;40:959.
[37] Weiss RA, Ghebremeskel Y, Charbonneau L. Polymer 2000;41:3471.
[38] Vallejo FJ, Eguiazabal JI, Nazabal J. Polymer 2000;41:6311.
[39] Ide F, Hasegawa A. J Appl Polym Sci 1974;18(4):963.
[40] Hong SM, Kim BC, Kim KU, Chung IJ. Polym J 1991;23:1347.
[41] Golovoy A, Kozlowski M, Narkis M. Polym Engng Sci 1992;32:854.
[42] Charoensirisomboon P, Saito H, Inoue T, Weber M, Koch E. Macromolecules 1998;31:4963.
[43] Koriyama H, Oyama HT, Ougizawa T, Inoue T, Weber M, Koch E. Polymer 1999;40:6381.
[44] Charoensirisomboon P, Chiba T, Torikai K, Saito H, Ougizawa T, Inoue T, Weber M. Polymer 1999;40:6965.
[45] Charoensirisomboon P, Inoue T, Weber M. Polymer 2000;41:4483.
[46] Charoensirisomboon P, Inoue T, Weber M. Polymer 2000;41:5977.
[47] Charoensirisomboon P, Inoue T, Solomko SI, Sigalov GM, Weber M. Polymer 2000;41:7033.
[48] Wu S. Polymer interface and adhesion. New York: Marcel Dekker, 1982.
[49] Chiang CR, Chang FC. Polymer 1997;38:4807.